KSCE Journal of Civil Engineering (2015) 19(6):1604-1611
DOI 10.1007/s12205-014-0079-0

Environmental Engineering
pISSN 1226-7988, eISSN 1976-3808
www.springer.com/12205

Effect of Ionic Strength and Permeate Flux on Membrane Fouling: Analysis of Forces acting on Particle Deposit and Cake Formation

S. Vigneswaran* and Dae-Young Kwon**

Received February 17, 2014/Revised August 17, 2014/Accepted September 16, 2014/Published Online December 5, 2014

Abstract

In Cross-Flow Microfiltration (CFMF), suspended particles deposit to form a cake layer on the membrane surface, which provides a resistance to permeate flow. The cake resistance, which plays an important role on the performance of CFMF, is mainly determined by the packing porosity of the cake and, the physical and chemical properties of particles. This study aimed at understanding the porosity and the specific filtration resistance of the cake for a given condition. These properties have been studied using experiments under a constant permeate flux. Factors such as permeate flux and ionic strength were investigated in terms of the particles deposition and cake formation. This study also adopted a force balance model to predict the deposit rate of particles and then compare with the experimental results. Inter-particle forces (electric double layer repulsion force and Van der Waals attraction force) were incorporated into the calculation of cake structure (cake porosity and specific resistance) together with the equilibrium condition of hydrodynamic forces. The experimental results showed that the higher the permeate flux led to the greater amount of particles deposit and the denser structure of cake. The porosity of cake decreased with the increase in ionic strength (0~0.01 M) and then increased sharply afterwards (0.01~0.1 M). The hydrodynamic force balance model estimated well the tendency of variation in cake structure depending on the ionic strength.

Keywords: *cross-flow microfiltration, membrane fouling, cake resistance, porosity, particle deposit, ionic strength, permeate flux*

1. Introduction

One of the major drawbacks hindering the application of membrane processes in water and wastewater treatment is the reduction in the flux with time (below the theoretical capacity of the membrane). Under the conditions of Constant Transmembrane Pressure (TMP) and cross-flow velocity, the flux in CFMF declines to a steady-state value which can be as much as two orders of magnitude lower than the initial or clean water value (Wang, 2014; Kim, 2004). In general, the typical temporary variation of the flux is an initial rapid decrease followed by a long but slow and gradual flux decline till it reaches the steady-state flux (Bugge, 2012; Lin, 2006).

It is well known that membrane fouling is one of the main phenomena responsible for this flux decline. The fouling mechanism is extremely complicated. The fouling affects the performance of the membrane either by deposition of a layer onto the membrane surface or, by complete or partial blockage of the membrane pores. This changes the effective membrane pore size distribution (Baccin, 2005).

For most CFMFs, filter cake may form on the membrane surface. In such a condition, cake resistance that plays an important role in the performance of filtration is mainly determined by the packing porosity of the filter cake and the physical properties of particles. As a result, the essential step is to understand the porosity and the specific filtration resistance of filter cake for a given filtration condition (Dong, 2006).

A variety of hydrodynamic models have been proposed to study the mechanism and to predict the permeate flux of cross-flow microfiltration of above micron particles (Belfort, 1994; Blake, 1992; Aimar, 1991). However, several previous efforts have pointed out the importance of inter-particle forces on the properties of a filter cake. Sharma *et al*. have proposed a structural network model to study the effects of pressure and inter-particle forces on the structure and the permeability of clay filter cake (Sharma, 1991). Lu *et al*. have used the Brownian dynamic simulation method to simulate the packing structure of submicron particles on the membrane surface (Lu, 1989). From the simulation, they suggested that the most compact cake would be formed when the friction drag and the Brownian force are of the same order of magnitude.

McDonogh *et al*. (1984) assumed a tetrahedral packing

*Professor, Faculty of Engineering, School of Civil & Environmental Engineering, University of Technology Sydney, PO Box 123, Broadway, Sydney NSW 2007, Australia (E-mail: Saravanamuth.Vigneswaran@uts.edu.au)
**Member, Associate Professor, Dept. of Civil and Urban Engineering, Inje University, Gimhae 621-749, Korea (Corresponding Author, E-mail: dykwon@inje.ac.kr)

geometry in a filter cake. They considered the particle interactions in terms of double layer theory to discuss the charge effect on the permeate flux in cross-flow ultrafiltrations. The predicted results using their theory agreed with the experimental result over two orders of magnitude of the particle size (McDonogh, 1984). McDonogh *et al*. then introduced Tiller's empirical power function to estimate the distribution of local solid compressive pressure within a filter cake (McDonogh, 1992). They found that the charge effects were still very significant for particles as large as 0.1 μm in radius, and that the results obtained from experiments and the theory over an order of magnitude of particle size were in agreement. However, they claimed that a closely packed cake was formed when the solid compressive pressure exceeded the maximum repulsive pressure.

In this study, the particles deposition and the cake formation (porosity and specific resistance) for a various ionic concentration were obtained experimentally and theoretically. The experiments were performed under a constant permeate flux,in which a constant rate of particles deposition and a homogenous structure of cake could be obtained. A force balance model was adapted to predict the deposition rate of particle. Inter-particle forces (electric double layer repulsion force and Van der Waals attraction force) were incorporated into the calculation of cake structure (cake porosity and specific resistance) together with the equilibrium condition of hydrodynamic forces.

2. Methodology

The schematic diagram of an experimental set-up is shown in Fig. 1. Monodispersed suspension of spherical polystyrene latex particles (of pre-determined concentration) was delivered from a feedtank (equipped with a stirrer) to the CFMF cell by a variable speed tubing pump. Both the permeate and retentate lines were returned to the feed tank to maintain constant inlet concentration. The pressure of membrane was controlled by two valves and the transmembrane pressure drop was monitored by using a pressure transducer (Model 19-626A from Devar Inc.) at three points (P_1, P_2 and P_f) every two minutes. In all experiments, permeate flux was increased step by step 60, 120, 180 and 240 $Lm^{-2}h^{-1}$, which was kept constant for 20 min by the suction pump (Watson Marlow 505S). After each step of the permeate flux, the membrane was cleaned by higher crossflow velocity with closing the valve of permeate flux.

The dimensions of filtration channel in the CFMF cell are 6 cm, 0.6 cm and 0.036 cm of length, width and thickness respectively. The CFMF cell has 9 filtration channels and the total membrane area is $3.24 \times 10^{-3} m^2$. The solution was circulated (crossflow filtration) along the surface of the flat-plate membrane in the module in which the cells are sufficiently spaced. Thus, one could consider that they do not interfere to each other from mass transfer or hydrodynamic point of view. The membranes used were PVDF (polyvinyl flouride) membrane (MILLIPORE : Catalogue no. GVLP OMS 10) with nominal pore sizes of 0.2 μm. In each experiment, new membranes were used to obtain reproducible results.

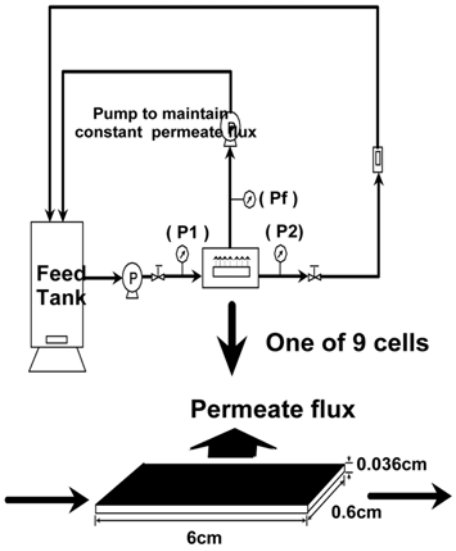

Fig. 1. Diagram of CFMF Experimental Set-up

Polystyrene latex particles of 3.2 μm were used in this study. They were larger than the membrane pore size to prevent particles from penetrating into the membrane pores. Influent concentration was monitored in terms of the turbidity of suspension in the feed tank in order to monitor the amount of particles' deposit on membrane. The turbidity of suspension was measured by a turbidimeter (2100P TURBIDIMETER, HACH). The specific density of the latex particles is 1.05 g/cm^3. A feed solution was prepared by adding a known amount of latex particles and potassium chloride (KCl) to control the particle concentration and the ionic strength of the solution respectively. Prefiltered distilled water was used to prepare the suspension. In the absence of KCl addition, the conductivity of a 50 mg/L latex particle suspension was equivalent to the 1×10^{-6} M KCl solution. Coulter counter (Delsa 440) was used to measure the zeta potential of the latex particle suspension at different ionic strength. The temperature was the ambient temperature (25 ± 2°C) and the pH was kept as 5.5~6.5 by adding HCl or NaOH in every experiment.

3. Result

3.1 Mass of Particle Deposit

Figure 2 presents the experimental results of deposited mass on the membrane surface with filtration time for different ionic strength values of 0, 0.001, 0.01 and 0.1 M, respectively. Each figure shows the tendency of particle deposit at constant values of permeate flux (60, 120, 180 and 240 $Lm^{-2}h^{-1}$). The figures show that the deposited mass increased with the increase in the permeate flux at all ionic strength values used. Higher permeate flux leads to a greater drag force to capture the particles down onto the membrane surface resulting in more deposit of particles (Baker, 1985). However, the rate of deposit was gradually

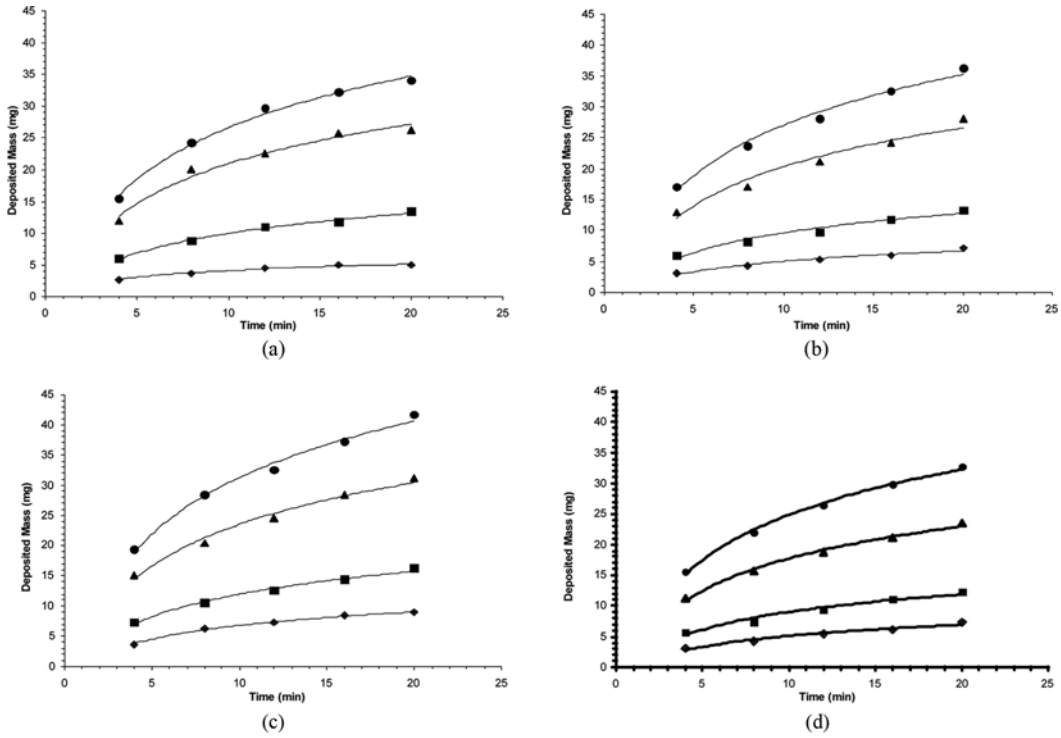

(◆: 60 L/m^{2}h, ■: 120 L/m^{2}h, ▲: 180 L/m^{2}h and ●: 240 L/m^{2}h)

Fig. 2. Deposited Mass at Different Ionic Strength of Constant Permeate Flux: (a) 0 M, (b) 0.00 M, (c) 0.01 M, (d) 0.1 M

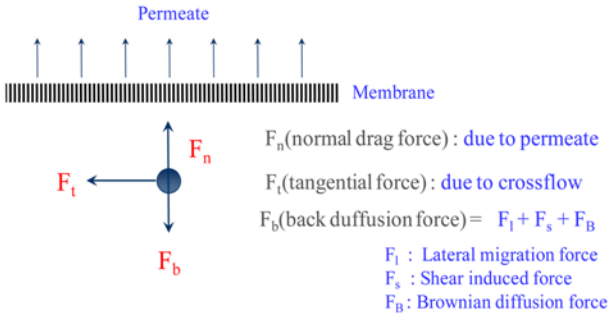

Fig. 3. Hydrodynamic Forces acting on Particle in Suspension

Table 1. Fraction of Deposited Mass

Permeate Flux (L/m^{2}h)	Percentage of deposited mass (%)*			
	0 M	0.001 M	0.01 M	0.1 M
60	38.1	55.8	69.1	49.4
120	52.7	54.7	65.9	57.6
180	73.9	82.3	92.2	85.8
240	83.9	90.3	95.6	86.9

* % of deposited mass = (mg of deposited particles)/(mg of particles in suspension) × 100

decreased with filtration time at all permeate flux, which meant that there was a limit mass of deposit for a certain permeate flux.

In general, forces acting on particle in suspension during the operation of CFMF are shown in Fig. 3. The deposit of particle on membrane surface depends on hydrodynamic forces - tangential force; F_t due to cross-flow parallel to membrane, normal drag force; F_n due to permeate flux perpendicular to membrane and back diffusion force; F_b (summation of lateral migration force, shear induced force and Brownian diffusion force). When the permeate flux was 60 or 120 Lm^{-2}h^{-1}, F_n was not great enough for particles to deposit compared to F_t and F_b. While F_n became great enough for particles to deposit when the permeate flux increased to 180 or 240 Lm^{-2}h^{-1}. The equilibrium of the hydrodynamic forces might also explain the gradual decrease in the rate of deposit with filtration time. A thicker layer of deposit after a certain filtration time made the space of membrane channel narrower, which resulted in great enough for F_t and F_b to stop the deposit.

The amount of particles deposited during each step of the permeate flux is presented in Table 1. For example, the deposited mass was 4.96 mg at the permeate flux of 60 Lm^{-2}h^{-1} for an ionic strength of 0M (after 20 min of constant flux membrane operation). The total amount of particles which would have in the suspension filtered through the membrane for the time was simply obtained from the data; influent concentration of 0.2 g/L, feed tank volume of 1 L, membrane surface area of 32.4 cm^2 and filtration time of 20 minutes. It led a fraction of the deposited mass out of the total amount of particles existed in the suspension to 38.1 %. Table 1 shows clearly that the increase in permeate flux resulted in the increase of particle deposit mass. When the permeate flux was 240 Lm^{-2}h^{-1}, more than 80% of particles in suspension were deposited. In particular, more than 90% of particles were deposited when ionic strength was 0.001 or 0.01 M. This result implies that advantage of CFMF such as

sweeping away due to tangential and back diffusion forces cannot be expected at high permeate flux. Table 1 also indicates that more deposition was obtained with the increase in ionic strength. Several researches reported that a particle has thicker diffuse-layer at lower ionic strength, which prevents the particle to deposit due to higher repulsive force (Lee, 2000; Kim, 2000). But, thinner diffuse-layer at higher ionic strength causes greater mass of particles to deposit due to less repulsive force.

It can be found from Table 1 that the deposit decreased suddenly at the ionic strength of 0.1 M. This sudden decrease might be due to the particles aggregation. Several researchers reported that this range of ionic strength (over 0.01 M) results in critical coagulation concentration (Bacchin, 2002; Lokjine, 1992). This aggregation of particles might cause a greater back diffusion effect on the particles. Thus, it prevents the particles from depositing onto the membrane surface.

3.2 Specific Resistance and Porosity

Figure 4 presents variations of TMP obtained from same experiments reported in Fig. 2. As can be seen in the figures, higher TMP was needed to obtain higher permeate flux. It can be explained by the Darcy's equation.

$$J = \frac{\Delta P}{\mu(R_m + R_f)} \tag{1}$$

where, J is a permeate flux, ΔP is TMP and μ is a fluid viscosity. R_m is an intrinsic membrane resistance which can be obtained from the clean water flux, and R_f is a fouling resistance.

Figure 4 also showed that TMP maintained constant below a certain flux (critical flux) but, it increased gradually above it (Kwon, 1998). This can be also explained by Darcy's equation. Under a constant permeate flux (J is constant in Eq. (1)), TMP is only a function of R_m and R_f. But, R_m is also constant because it is determined by the characteristics of membrane used. Therefore, TMP would be constant if no fouling occurs (R_f is 0). However, it would increase when fouling occurs ($R_f > 0$). From the experimental result in Fig. 4, the values of critical flux for 0, 0.001 and 0.01 M seemed to exist between 120 and 180 $Lm^{-2}h^{-1}$, while that for 0.1 M seemed to be between 180 and 240 $Lm^{-2}h^{-1}$. The pattern of variation of TMP was different at different ionic strength. This might be because different structures of cakes were formed at different ionic strength: specific resistance and porosity.

Assuming that R_f is caused by the particles deposition and the cake formation only, the Eq. (1) can be written as follows:

$$J = \frac{\Delta P}{\mu(R_m + \alpha M_d)} \tag{2}$$

where, α is a specific hydraulic resistance of the cake and M_d is a mass of deposited particles. The following equation can be used for the flow through a porous medium:

$$\Delta P = \frac{150(1-\varepsilon)^2}{d_p^2 \quad \varepsilon^3}\mu J z \tag{3}$$

where, ε and z are the porosity and the thickness of the cake respectively. The cake thickness z can be related to the deposited mass of M_d using the following equation:

$$z = \frac{M_d}{\rho_p(1-\varepsilon)A_m} \tag{4}$$

where, ρ_p is the density of deposited particles and A_m is the area

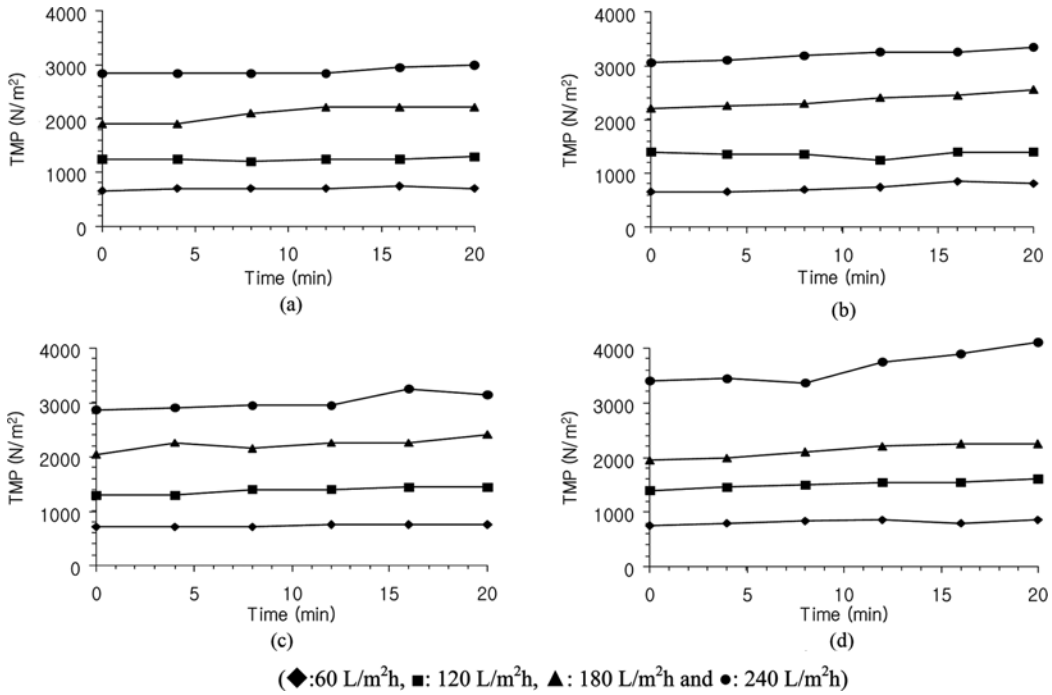

Fig. 4. Variation of TMP with Time at Different Permeate Flux: (a) 0 M, (b) 0.001 M, (c) 0.01 M, (d) 0.1 M

Table 2. Specific Resistance and Porosity Of Cake at Different Ionic Strength and Permeate Flux

Flux (L/m^{2}h)	0 M		0.001 M		0.01 M		0.1 M	
	α ($\times 10^9$ m/kg)	ε (%)	α ($\times 10^9$m/kg)	ε (%)	α ($\times 10^9$m/kg)	ε (%)	α ($\times 10^9$m/kg)	ε (%)
60	0.053	0.93	4.09	0.85	5.48	0.82	3.3	0.87
120	4.09	0.85	15.8	0.69	19.8	0.66	11.6	0.73
180	7.82	0.78	48.9	0.54	131	0.42	15.8	0.69
240	28.8	0.61	120	0.43	230	0.36	52.9	0.53

The unit of the specific resistance of the cake is m/kg

Table 3. Equations of Hydrodynamic and Inter-Particle Forces

Hydrodynamic forces	$F_l = 1.7009(3\pi)\mu d_p\left\{6\frac{d_p}{2L}\left[1-\left(\frac{d_p}{2L}\right)\right]u_s\right\}$
	$F_n = 3\pi\mu d_p u_p\left\{\frac{R_m d_p}{3}+(1.072)^2\right\}^{0.5}$
	$F_b = 3\pi\mu d_p(u_l+u_s+u_b)\left\{\frac{R_m d_p}{3}+(1.072)^2\right\}^{0.5}$
	$u_l = \frac{2.6u_s^2 d_p^3\rho}{16\mu L^2},\ u_s = \frac{u_s d_p^2}{20L^2},\ u_b = \frac{kT}{3\pi\mu L d_p}$
	μ: the suspended viscosity, d_p: the particle diameter,
	u_p: permeate flux, R_m: intrinsic membrane resistance
	u_l: lateral migration velocity, u_s: shear-induced velocity
	u_b: Brownian diffusion velocity, u_s: average cross-flow velocity
	ρ: particle density, L: channel clearance
	k: Boltzman constant (1.38 × 10 − 23 J/K), T: temperature.
Inter-particle forces	$F_e = 4\pi e_0 e_r\frac{d_p^2}{(D+2d_p)^2}\varphi^2\exp(-kD)(1+k(D+2d_p))$
	$k = \left(\frac{2\times 10^3 e^2 N_A I}{e_o e_r kT}\right)^{0.5}$
	$F_v = -\frac{A_H d_p}{12D^2}\left(1-\frac{1}{1+\frac{\lambda}{cD}}\right)$
	e_0 (=8.85 ×10-12C2/Jm): absolute permitivity of free space
	e_r: dielectric constant of the liquid between particles,
	φ: zeta potential of particles
	k: reciprocal of the thickness of the double layer
	e: electrical charge (=1.6 × 10-19 C)
	N_A: Avogadro's number (=6.022 × 1023)
	I: ionic strength (mol/L).
	A_H: Hamaker constant
	λ: characteristic wavelength for the interaction
	D: distance between particles

of the membrane covered by the deposited particles. Substituting Eqs. (4) into (3), one obtains:

$$\Delta P = \frac{150(1-\varepsilon)}{d_p^2}\frac{}{\varepsilon^3}\mu J\frac{M_d}{\rho_p A_m} \quad (5)$$

Using the values of J, M_d (presented in Fig. 2) and ΔP (presented in Fig. 3) measured from the experiments, the above Eqs. (1) to (6) are solved for the specific resistance α and the porosity ε of the cake. The results obtained are presented in Table 2.

The specific resistance was increased with the increase in

permeate flux at all cases of ionic strength. However, it showed significantly different values at different ionic strength. At 0 M, it increased from 0.55×10^9 to 28.8×10^9 m/kg when the permeate flux increased from 60 to 240 $Lm^{-2}h^{-1}$. While it increased up to 120×10^9 and 230×10^9 m/kg from 4.09×10^9 and 5.48×10^9 for the cases of 0.001 and 0.01 M, respectively. The high increase was due to compact cake porosity as well as high deposit mass. As can be seen in Table 3, porosity decreased up to 0.43 and 0.36 at the cases of 0.001 and 0.01 M, respectively. The increase in ionic strength from 0.01 to 0.1 M resulted in decrease in specific resistance. This resulted from the growth of particle size due to particles' aggregation. The bigger particles in the cake caused the bigger porosity as shown in Table 3.

The effect of ionic strength on the structure of cake can be explained by the forces acting on particles in the cake. Fig. 5 shows double layer repulsive force; F_e and van der Waals attractive force; F_v as well as hydrodynamic forces. In general, lower ionic strength such as 0 M makes cake structure loose resulted from relatively higher F_e and lower F_v (Field, 1995). But, the cake structure becomes compact due to relatively lower F_e and higher F_v when the ionic strength is higher such as 0.001 and 0.01 M.

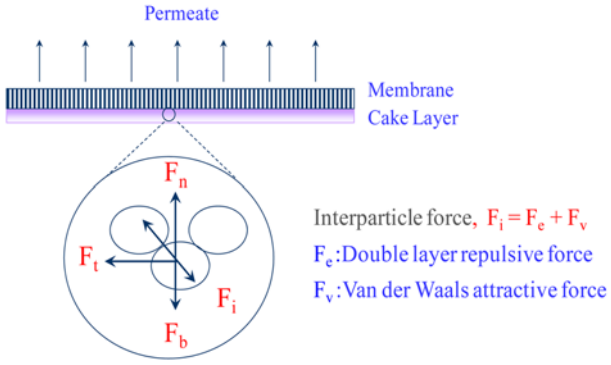

Fig. 5. Forces acting on Particles in Cake Layer

4. Discussion

During the operation of CFMF, particles in suspension are transported by liquid towards membrane surface and deposit on the membrane to form a filter cake. The deposit of particle depends on hydrodynamic forces. If normal drag force caused by permeate flux is greater than tangential and back diffusion forces, the particle would deposit and form a cake. The main forces acting on the cake are the hydrodynamic forces and the inter-particle forces. The tangential force due to cross-flow of the suspension can be assumed to be only acting on the surface of the cake. The gravity is negligible compared to the other forces in the case of filtration of submicron and micron sized particles. The hydrodynamic forces and inter-particle forces were obtained from literature review and listed in Table 3 ((McDonogh, 1992; O'Neill, 1968; Goren, 1979; Green, 1980).

Specific filtration resistance of the cake can be related to the porosity of the formed cake as follows:

$$\alpha = kS_0^2 \frac{(1-\varepsilon)}{\varepsilon^3 \rho_p} \tag{6}$$

where, S_0 is the specific surface area of particles. Since the Kozeny constant k is given as:

$$k = \frac{2\varepsilon^3}{(1-\varepsilon)[Ln\{1/(1-\varepsilon)\} - \{1-(1-\varepsilon)^2\}/\{1+(1-\varepsilon)^2\}]} \tag{7}$$

Here, k is a function of e, the value of k should be calculated in accordance with the change in the value of the porosity. Once the porosity of the cake and the values of k, S_0 and ρ_p are known, the value of the corresponding specific filtration resistance in the cake can be estimated from Eq. (7).

Figure 6 presents the inter-particle forces at various particle-particle distance for particle size of 3.2 μm at different ionic strength. From these values, the equilibrium particle-particle distance for a given condition can be obtained. The calculation was based on the idea that the inter-particle force should be equal

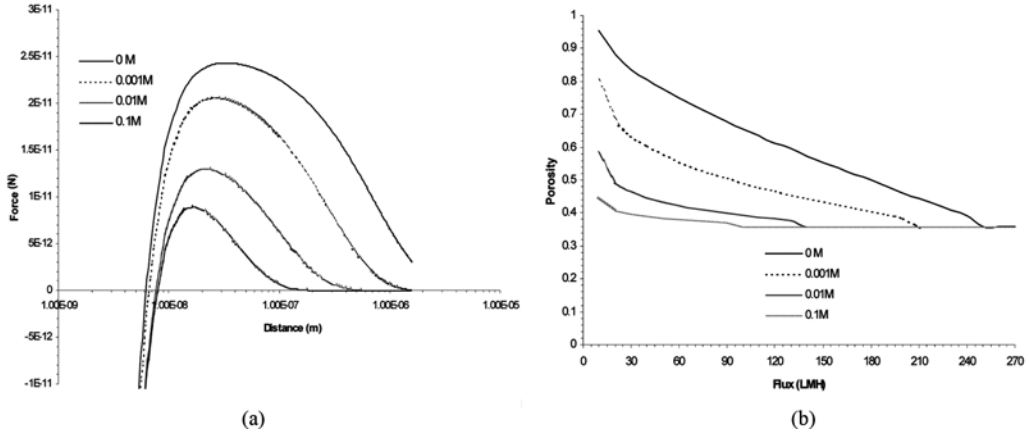

Fig. 6. Calculated Inter-Particle Force and Porosity at various Particle-Particle Distance (Hamarker Constant = 10^{-20} J, λ=10^{-7}, c = 5.32) and Theoretical Values of the Porosity at Different Permeate Flux Values and at Different Ionic Strength: (a) Inter-Particle Force, (b) Porosity

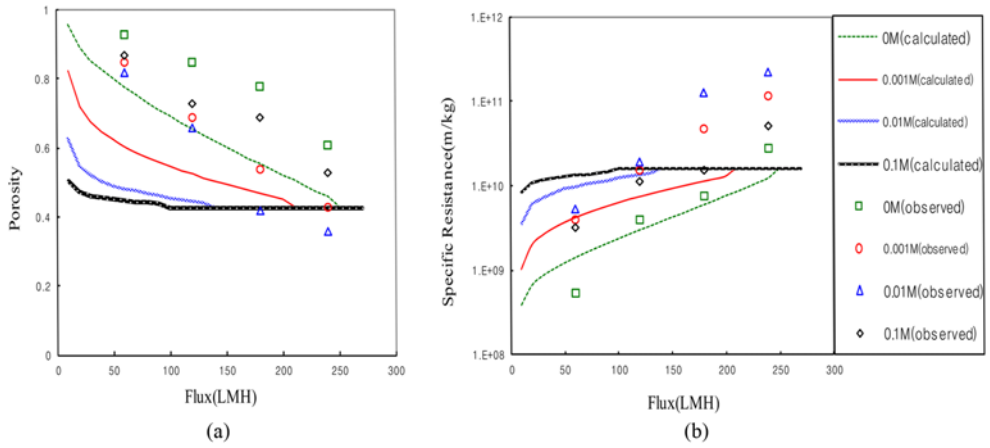

Fig. 7. Calculated and Observed Values of Porosity and Specific Resistance at various Permeate Flux: (a) Porosity, (b) Specific Resistance

to the total hydrodynamic forces. Then, the porosity of the cake for a given condition can be calculated and the specific resistance of the cake was then calculated. The calculated values of porosity and specific resistance were compared to the observed ones from the experiments in Figs. 7(a) and 7(b), respectively. Structures of the cake such as porosity and specific resistance were well estimated by the analysis of hydrodynamic and inter-particle forces. However, there was no consideration on the particles' aggregation over 0.01 M of ionic strength resulting in a significant difference between the calculated and the observed values in the case of 0.1 M ionic strength.

5. Conclusions

From a series of cross-flow microfiltration experiments conducted under a constant permeate flux, deposit and cake formation (porosity and the specific resistance of the cake) was obtained for different ionic strength. A hydrodynamic packing model was also formulated to predict the cake structure. The model incorporates the inter-particle forces (electric double layer repulsive force and van der Waals attractive force) into a hydrodynamic force balance model. From the investigation of the permeate flux and the ionic strength on the particle deposit and cake structure, the followings were concluded :

1. The higher the permeate flux, the greater the tendency of particles deposition (for a flux range of 60~240 $Lm^{-2}h^{-1}$). At lower permeate flux (for example, 60 $Lm^{-2}h^{-1}$), a significant amount of particles in the suspension filtered (more than 50%) did not deposit on the membrane. This implies that there would be a flux below which there is no particles deposit. The higher permeate flux, the denser the cake formed (higher specific resistance and smaller porosity)
2. The porosity decreased with the increase in ionic strength (for a ionic strength range of 0~0.01 M) and then increased sharply afterwards in the experiments. But, the model results showed a constant decrease in an ionic strength range of 0 to 0.1 M
3. The hydrodynamic force balance model estimated well the tendency of variation in cake structure depending on the ionic strength of water except for the one at the ionic strength of 0.1 M

Acknowledgements

This work (Grants No. C0142152) was supported by Business for Cooperative R&D between Industry, Academy, and Research Institute funded Korea Small and Medium Business Administration in 2013.

References

Aimar, P. and Howell, J. A. (1991). "Concentration polarization build-up in hollow fibers: A method of measurement and its modeling in ultrafiltration." *J. Mem. Sci.*, Vol. 59, Issue 1, pp. 81-99, DOI: 10.1016/S0376-7388(00)81223-5.

Baccin, P., Espinasse, B., and Aimar, P. (2005). "Distribution of critical flux: Modeling, experimental analysis and consequences for cross-flow membrane filtration." *J. Mem. Sci.*, Vol. 250, Issues 1-2, pp. 223-234, DOI: 10.1016/j.memsci.2004.10.033.

Bacchin, P., Si-Hassen, D., Starov, V, Clifton, M. J., and Aimar, P. (2002). "A unifying model for concentration polarization, gel-layer formation and particle deposition in cross-flow membrane filtration of colloidal suspensions." *Chem. Eng. Sci.*, Vol. 57, Issue 1, pp. 77-91, DOI: 10.1016/S009-2509(01)00316-5.

Baker, R. J., Fane, A. J., Fell, C. J. D., and Yoo, B. H. (1985). "Factors affecting flux in crossflow filtration." *Desalination*, Vol. 53, Issues 1-3, pp. 81-93, DOI: 10.1016/0011-9164(85)85053-0.

Belfort, G., Davis, R. H., and Zydey, A. L. (1994). "The behavior of suspensions and macromolecular solutions in crossflow microfiltration." *J. Mem. Sci.*, Vol. 96, Issues 1-2, pp. 1-58, DOI: 10.1016/0376-7388(94)00119-7.

Blake, N. J., Cumming, I. W., and Streat, M. (1992). "Prediction of steady state crossflow filtration using a force balance model." *J. Mem. Sci.*, Vol. 68, Issue 3, pp. 205-216, DOI: 10.1016/0376-7388(92)85022-13.

Bugge, T. V., Jorgensen, M. K., Christensen, M. L., and Keiding, K. (2012). "Modeling cake buildup under TMP-step filtration in a

membrane bioreactor: Cake compressibility is significant." *Water Res*., Vol. 46, Issue 14, pp. 4330-4338, DOI: 10.1016/j.watres. 2012.06.015.

Dong, C., Linda, K. W., Harold, W. W., and Lenhart, J. J. (2006). "Ultrasonic control of ceramic membrane fouling caused by natural organic matter and silica particles." *J. Mem. Sci*., Vol. 276, Issues 1-2, pp. 135-144, DOI: 10.1016/j.memsci.2005.09.039.

Field, R. W., Wu, D., Howell, J. A., and Gupta, B. B. (1995). "Critical flux concept for microfiltration fouling." *J. Mem. Sci*., Vol. 100, Issue 3, pp. 259-272, DOI: 10.1016/0376-7388(94)00265-Z.

Goren, S. L. (1979). "The hydrodynamic force resisting the approach of a plane permeable wall." *J. Colloid Interface Sci*., Vol. 69, Issue 1, pp. 78-85, DOI: 10.1016/0021-9797(79)90082-1.

Green, G. and Belfort, G. (1980). "Fouling of ultrafiltration membranes : Lateral migration and the particle trajectory model." *Desalination*, Vol. 35, pp. 129-147, DOI: 10.1016/S0011-9164(00)88607-5.

Kim, S. H. and Park, H. K. (2000). "Prediction of critical flux conditions in crossflow microfiltration using a numerical model." *Journal of the Korean Society of Civil Engineers*, KSCE, Vol. 20, No. 1B, pp. 131-138.

Kim, S. H. and Park, H. K. (2004). "Reduction of cake layer by re-aggregation at the movable cake layer in coagulation-crossflow microfiltration process." *Journal of the Korean Society of Civil Engineers,* KSCE, Vol. 24, No. 2B, pp. 147-154.

Kwon, D. Y. (1998). Experimental investigation on critical flux in cross-flow microfiltration, PhD Thesis, UTS.

Lee, J. D., Lee, S. H., Jo, M. H., Park, P. K., Lee, C. H., and Kwak, J. W. (2000). "Effect of coagulation conditions on membrane filtration characteristics in coagulation-microfiltration process for water treatment." *Environ. Sci. Technol*., Vol. 34, No. 17, pp. 3780-3788, DOI: 10.1021/es9907461.

Lin, C. J., Shirazi, S., Rao, P., and Agarwal, S. (2006). "Effect of operational parameters on cake formation of $CaSO_4$ in nanofiltration." *Water Res*., Vol. 40, Issue 4, pp. 806-816, DOI: 10.1016/j.watres. 2005.12.013.

Lokjine, M. H., Field, R. W., and Howell, J. A. (1992). "Crossflow filtration of cell suspensions: A review of models with emphasis on particle size effects." *Trans. I Chem. E.*, Vol. 70, Part C, pp. 149-161.

Lu, W. M. and Ju, S. C. (1989). "Selective particle deposition in crossflow filtration." *Sep. Sci, & Tech*., Vol. 24, Issues 7-8, pp. 517-540.

McDonogh, R. M., Fell, C. J. D., and Fane, A. G. (1984). "Surface charge and permeability in the ultrafiltration of non-flocculating colloids." *J. Mem. Sci*., Vol. 21, Issue 3, pp. 285-294, DOI: 10.1016/S0376-7388(00)80219-7.

McDonogh, R. M., Welsch, K., Fell, C. J. D., and Fane, A. G. (1992). "Incorporation of the cake pressure profiles in the calculation of the effect of particle charge on the permeability of filter cakes obtained in the filtration of colloids and particulates." *J. Mem. Sci*., Vol. 72, Issue 3, pp. 197-204, DOI: 10.1016/0376-7388(92)80200-4.

O'Neill, M. E. (1968). "A sphere in contact with a plane wall in a slow linear shear flow." *Chem. Eng. Sci*., Vol. 23, Issue 11, pp. 1293-1298, DOI:10.1016/0009-2509(68)89039-6.

Sharma, M. M. and Lei, Z. (1991). "A model for clay filter cake properties." *Colloids Surf*., Vol. 56, pp. 357-381, DOI: 10.1016/0166-6622(91)80132-8.

Wang, X. M. and Li, X. Y. (2014). "Modeling of the initial deposition of individual particles during the cross-flow membrane filtration." *Colloids & Surfaces A: Physicochem. Eng. Aspects,* Vol. 440, pp. 91-100, DOI: 10.1016/j.colsurfa.2012.10.033.